Eur. Phys. J. C (2016) 76:491
DOI 10.1140/epjc/s10052-016-4324-1

THE EUROPEAN PHYSICAL JOURNAL C

Regular Article - Theoretical Physics

Reconstructions of $f(T)$ gravity from entropy-corrected holographic and new agegraphic dark energy models in power-law and logarithmic versions

Pameli Saha[a], **Ujjal Debnath**[b]

Department of Mathematics, Indian Institute of Engineering Science and Technology, Shibpur, Howrah 711 103, India

Received: 6 June 2016 / Accepted: 9 August 2016 / Published online: 7 September 2016

Abstract Here, we peruse cosmological usage of the most promising candidates of dark energy in the framework of $f(T)$ gravity theory where T represents the torsion scalar teleparallel gravity. We reconstruct the different $f(T)$ modified gravity models in the spatially flat Friedmann–Robertson–Walker universe according to entropy-corrected versions of the holographic and new agegraphic dark energy models in power-law and logarithmic corrections, which describe an accelerated expansion history of the universe. We conclude that the equation of state parameter of the entropy-corrected models can transit from the quintessence state to the phantom regime as indicated by recent observations or can lie entirely in the phantom region. Also, using these models, we investigate the different areas of the stability with the help of the squared speed of sound.

1 Introduction

The type Ia Supernovae and cosmic microwave background (CMB) [1,2] observations point out that our universe is precisely accelerating, which is caused by some unknown fluid having positive energy density and negative pressure, called "Dark Energy" (DE). Observations indicate that dark energy occupies about 70 % of the total energy of the universe, whereas the contribution of dark matter is 26 % and the rest 4 % is baryonic matter. For related review works see Refs. [3,4]. Although a long-time argument has been made on this interesting issue of modern cosmology, we still have little knowledge about DE. The cosmological constant Λ is the most appealing and simplest candidate for DE which obeys the equation of state parameter $w = -1$. However, the cosmological constant suffers from two serious theoretical problems, i.e., the cosmological constant problem and the coincidence problem. In this respect, different dynamical DE models and different modified theories of gravity have been developed. Moreover, the reconstruction phenomenon of different DE models [5–8] is gaining great attention in the discussion of the accelerated expansion of the universe.

In recent years, an interesting idea has been proposed: to study the dark energy in the new form, i.e., the Holographic Dark Energy (HDE) model [9–11], which arises from the holographic principle [12] stating that the number of degrees of freedom of a physical model must be finite [13] and an infrared cut-off should constrain it [14]. In quantum field theory [14], for developing a black hole , the UV cut-off Λ should relate with the IR cut-off L due to the limit set. In Ref. [15] Li debated the relation $L^3\rho_\Lambda \leq LM_P^2$, where ρ_Λ is the quantum zero point energy density and $M_P = \frac{1}{\sqrt{8\pi G}}$ is the reduced Planck mass, i.e., the mass of a black hole of the size L should not be exceeded by the total energy in a region of same size. The HDE models have been discussed in [16–20]. The black hole entropy $S_{\rm BH}$ plays an important role in the simplification of HDE, given as usually, $S_{\rm BH} = \frac{A}{4G}$, where $A \sim L^2$ is the area of the horizon.

The power-law corrections arise in dealing with the entanglement of quantum fields moving into and out of the horizon [21–23], for which the entropy–area relation for a power-law correction can be given as

$$S_{\rm BH} = \frac{A}{4G}[1 - K_\epsilon A^{1-\frac{\epsilon}{2}}], \tag{1}$$

where

$$K_\epsilon = \frac{\epsilon(4\pi)^{\frac{\epsilon}{2}-1}}{(4-\epsilon)r_c^{2-\epsilon}}.$$

[a] e-mail: pameli.saha15@gmail.com
[b] e-mail: ujjaldebnath@gmail.com

Here, r_c is the crossover scale and ϵ is the dimensionless constant. Motivated by this corrected entropy–area relation (1) in the setup of LQG (loop quantum gravity), Wei [24] suggested the energy density of the ECHDE in power-law correction.

Also the entropy–area relation for a logarithmic correction can be improved to [25–28]

$$S_{\rm BH} = \frac{A}{4G} + \alpha \ln\left[\frac{A}{4G}\right] + \beta, \tag{2}$$

where α and β are dimensionless constants of order unity. Recently, inspired by the corrected entropy–area relation (2) in the setup of LQG, Wei [24] propounded the energy density of the entropy-corrected HDE (ECHDE) in logarithmic correction.

From quantum mechanics along with the gravitational purpose in general relativity, another type of dark energy is the agegraphic DE (ADE) model. The original agegraphic DE model was presented by Cai [29] to study the accelerating expansion of the universe where the age (T) of the universe is present in the expression of the energy density, given by

$$\rho_\Lambda = 3c^2 M_P^2 T^{-2}. \tag{3}$$

The numerical factor $3c^2$ is used to recover some uncertainties. Subsequently, Wei and Cai [30] suggested a new kind of ADE model by removing the age of the universe and replacing it with the conformal time (η), called the new agegraphic DE (NADE) model. Recently, Wei [24] initiated the energy density of the entropy-corrected NADE (ECNADE) in power-law and logarithmic corrections like the entropy-corrected HDE (ECHDE) in a power-law and a logarithmic correction model and details of these were discussed in [31–35].

There is an another discussion for the cosmic acceleration of the universe (predicted from observational data), the so-called "modified gravity" where we do not require any additional components like DE (for a review see [36]) for the acceleration of the universe. Various kinds of modified theories have been proposed such as the $f(R)$ [38], $f(G)$ [39,40], Horava–Lifshitz [41] and Gauss–Bonnet [42,43] theories of gravity. Recently, [44,45] formulated a new kind of theory of gravity known as $f(T)$ gravity in a space-time possessing absolute parallelism. $f(T)$ gravity has been recently studied in [46,47]. In the $f(T)$ theory of gravity, the teleparallel Lagrangian density gave a description of the torsion scalar T, using a function of T, i.e., $f(T)$, for the late-time cosmic acceleration [48]. In a recent work, Jamil et al. [49,50] investigated the interacting DE model and state-finder diagnostic in $f(T)$ cosmology.

Recently, the reconstruction of various types of modified gravities $f(R)$, $f(T)$, $f(G)$, Einstein–aether etc. with the various dark energy models have made a plea topic in cosmology [51–55]. Farooq et al. [56] reconstructed $f(T)$ and $f(R)$ gravity according to (m, n)-type holographic dark energy, Karami et al. [57] did the reconstruction of $f(R)$ modified gravity from ordinary and entropy-corrected versions of holographic and new agegraphic dark energy models and also Debnath [58] discussed the topic of reconstruction of $f(R)$, $f(G)$, $f(T)$, and Einstein–aether gravities from entropy-corrected (m, n) type pilgrim dark energy. Motivated by these works, with the help of modified $f(T)$ gravity and considering the entropy-corrected versions of the HDE and NADE scenarios, it is interesting to investigate how the $f(T)$-gravity can describe ECHDE and ECNADE densities in power-law and logarithmic versions as effective theories of DE models.

This paper is arranged as follows. In Sect. 2, we give a brief idea of the theory of $f(T)$ gravity and corresponding solutions for a FRW background. In Sects. 3 and 4, we reconstruct the different $f(T)$ gravity models, i.e., we find an unknown function $f(T)$ corresponding to the ECHDE and ECNADE models in the power-law and logarithmic versions, respectively, and analyze the EoS parameter for the corresponding models. Karami et al. [59] also investigated the modified teleparallel gravity models as an alternative for holographic and new agegraphic dark energy models. In Sect. 5, we provide the analysis and comparison of the reconstructed models. Section 6 is devoted to our conclusions.

2 The brief idea of $f(T)$ gravity and ECHDE in power-law and logarithmic correction

Teleparallel gravity is correlated with a gauge theory for the translation group. For the unusual character of these translations, any gauge theory with these translations is different from the usual gauge theory in many ways, mostly in the background of a tetrad field, whereas this field is used to define a linear Weitzenbock connection, presenting torsion without curvature. For the details of this gravity theory see the review [60]. We consider here how to generalize the teleparallel Lagrangian T to a function $f(T) = T + g(T)$, which is the same as the generalization of the Ricci scalar in Einstein–Hilbert action to the modified $f(R)$ gravity. We can write the action of $f(T)$ gravity, coupled with matter, L_m, by [61–65]

$$S = \frac{1}{16\pi G}\int {\rm d}^4 x e(T + g(T) + L_m) \tag{4}$$

where $e = det(e^i_\mu) = \sqrt{-g}$. Now we will take the units $8\pi G = c = 1$. Here, the teleparallel Lagrangian T, known as the torsion scalar, is defined as follows:

$$T = S^{\mu\nu}_\rho T^\rho_{\mu\nu}, \tag{5}$$

where

$$T^{\rho}_{\mu\nu} = e^{\rho}_{i}\left(\partial_{\mu}e^{i}_{\nu} - \partial_{\nu}e^{i}_{\mu}\right), \tag{6}$$

$$S^{\mu\nu}_{\rho} = \frac{1}{2}(K^{\mu\nu}_{\rho} + \delta^{\mu}_{\rho}T^{\theta\nu}_{\theta} - \delta^{\nu}_{\rho}T^{\theta\mu}_{\theta}), \tag{7}$$

and $K^{\mu\nu}_{\rho}$ is the contorsion tensor

$$K^{\mu\nu}_{\rho} = -\frac{1}{2}(T^{\mu\nu}_{\rho} - T^{\nu\mu}_{\rho} - T^{\mu\nu}_{\rho}). \tag{8}$$

Making a variation of the action with respect to the vierbein e^{i}_{μ}, we get the field equations:

$$e^{-1}\partial_{\mu}\left(eS^{\mu\nu}_{i}\right)(1+g_{T}) - e^{\lambda}_{i}T^{\rho}_{\mu\lambda}S^{\nu\mu}_{\rho}g_{T} + S^{\mu\nu}_{i}\partial_{\mu}(T)g_{TT} - \frac{1}{4}e^{\nu}_{i}(1+g(T)) = \frac{1}{2}e^{\rho}_{i}\Upsilon^{\nu}_{\rho}, \tag{9}$$

where g_T and g_{TT} are the first and second derivatives of g with respect to T. Here $\Upsilon_{\rho\nu}$ is the stress tensor. Now we assume the usual spatially flat metric of the Friedmann–Robertson–Walker (FRW) universe giving the line element written as

$$\mathrm{d}s^2 = \mathrm{d}t^2 - a^2(t)\sum_{i=1}^{3}(\mathrm{d}x^i)^2 \tag{10}$$

where $a(t)$ is the scalar factor, a function of the cosmic time t. Moreover, we consider the background to be a perfect fluid. Using the FRW metric and the perfect fluid matter in the Lagrangian (5) and the field equation (9), we obtain

$$T = -6H^2, \tag{11}$$

$$3H^2 = \rho - \frac{1}{2}g - 6H^2g_T, \tag{12}$$

$$-3H^2 - 2\dot{H} = p + \frac{1}{2}g + 2(3H^2+\dot{H})g_T - 24\dot{H}H^2g_{TT}, \tag{13}$$

where ρ and p are the energy density and pressure of ordinary matter content of the universe, respectively. The Hubble parameter (H) is defined as $H = \frac{\dot{a}}{a}$, where the "dot" denotes the derivative with respect to the cosmic time. Equation (11) shows that $T < 0$.

The equation of state (EoS) parameter due to the torsion contribution is defined as

$$w_{\Lambda} = \frac{p_{\Lambda}}{\rho_{\Lambda}}, \tag{14}$$

which shows the phantom, $w_{\Lambda} < -1$, and quintessence, $w_{\Lambda} > -1$, dominated universe.

We define the redshift z as

$$1 + z = \frac{a_0(t)}{a(t)}$$

where $a_0(t) = 1$ for the present epoch.

For a given $a(t)$, with the help of Eqs. (12) and (13) one can reconstruct the $f(T)$ gravity according to any DE model given by the EoS $p_{\Lambda} = p_{\Lambda}(\rho_{\Lambda})$, i.e., $\rho_{\Lambda} = \rho_{\Lambda}(a)$. There are two classes of scale factors which one usually considers for describing the accelerating universe in $f(R)$, $f(T)$, etc.

Class I The first class of scale factor is given by [66],

$$a(t) = a_0(t_s - t)^{-n},\ t \le t_s \tag{15}$$

where a_0, n are constants and t_s defines the future singularity time. Hence,

$$H = \frac{n}{t_s - t}, \tag{16}$$

$$T = -\frac{6n^2}{(t_s - t)^2}. \tag{17}$$

Class II For the second class of scale factor defined as [66],

$$a(t) = a_0t^n, n > 0. \tag{18}$$

One obtains

$$H = \frac{n}{t}, \tag{19}$$

$$T = -\frac{6n^2}{t^2}. \tag{20}$$

For both cases we get

$$z = \left(n\sqrt{\frac{6}{-T}}\right)^n - 1. \tag{21}$$

Using the two classes of scale factors (15) and (18), we reconstruct the different $f(T)$ gravities according to the ECHDE and ECNADE models in power-law and logarithmic versions.

3 $f(T)$ reconstruction from ECHDE in a power-law and a logarithmic correction models

3.1 ECHDE in power-law correction

Reference [24] proposed the energy density of the ECHDE in power-law correction using the relation (1) [24],

$$\rho_{\Lambda} = 3\delta^2R_h^{-2} - \lambda R_h^{-\epsilon} \tag{22}$$

where λ is a constant related with ϵ and K_{ϵ}, δ is a constant. In the special case $\lambda = 0$, the above equation reduces to the well-known HDE density. Also R_h is the future event horizon defined as

$$R_h = a\int_{t}^{t_s}\frac{\mathrm{d}t}{a}. \tag{23}$$

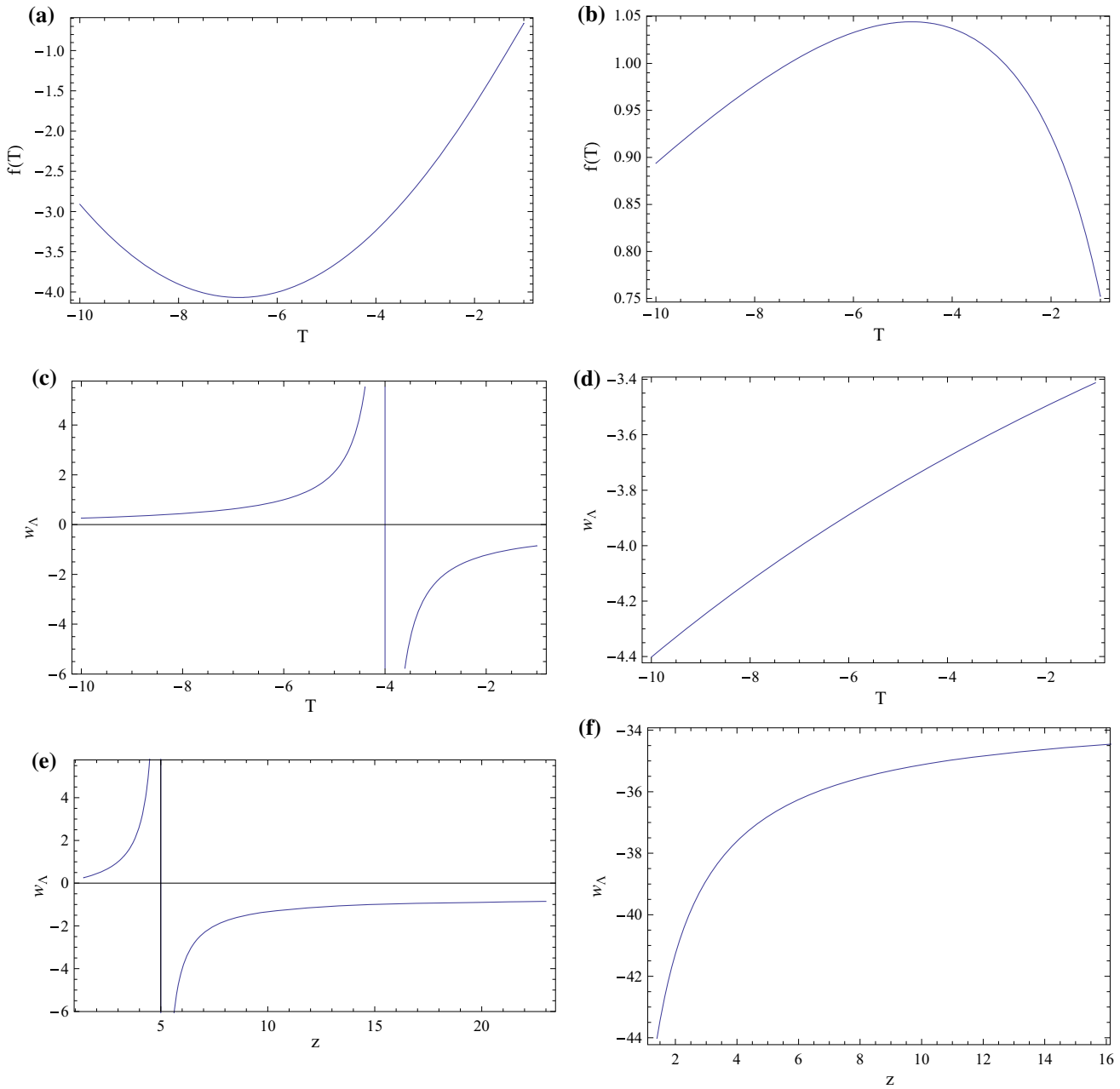

Figs. 1–6 **a, c, e** Plots of $f(T)$ and w_Λ for class I scale factor in ECHDE $f(T)$ gravity in a power-law correction model. **b, d, f** Plots of $f(T)$ and w_Λ for class II scale factor in ECHDE $f(T)$ gravity in a power-law correction model

For the first class (class I) of the scale factor (15) and using Eq. (16), the future event horizon R_h yields

$$R_h = a(t)\int_t^{t_s}\frac{\mathrm{d}t}{a(t)} = \frac{t_s - t}{n+1} = \sqrt{-\frac{6n^2}{T(n+1)^2}}. \tag{24}$$

Substituting Eq. (24) into (22) one can get

$$\rho_\Lambda = \frac{\delta^2(n+1)^2(-T)}{2n^2} - \lambda\left(\frac{n+1}{\sqrt{6}n}\right)^{\epsilon}(-T)^{\frac{\epsilon}{2}}. \tag{25}$$

Substituting Eq. (25) in the differential equation (12), i.e., $\rho = \rho_\Lambda$, gives the following solution

$$f(T) = c\sqrt{-T} - \frac{\delta^2(n+1)^2(-T)}{n^2} + \frac{2\lambda}{(\epsilon-1)}\left(\frac{n+1}{\sqrt{6}n}\right)^{\epsilon}(-T)^{\frac{\epsilon}{2}} \tag{26}$$

where c is the integration constant to be determined from the necessary boundary condition. In Fig. 1–6, we understand that $f(T) \nrightarrow 0$ as $T \to 0$ for the solution obtained

from Eq. (26). We also observe that $f(T)$ first decreases and then increases as T increases keeping in mind that $f(T)$ takes always a negative value for all values of negative T. Substituting Eq. (26) into (13) and using (25) we obtain the EoS parameter of the ECHDE $f(T)$ gravity in a power-law correction model as $w_\Lambda = \frac{p_\Lambda}{\rho_\Lambda}$ graphically. In Fig. 1–6, we see that the EoS parameter can justify the transition from the quintessence state, $w_\Lambda > -1$, to the phantom regime, $w_\Lambda < -1$, i.e., it crosses the phantom divide line $w_\Lambda = -1$ if we draw the graph of the EoS parameter with T and z using Eq. (21), respectively. So in this case, $f(T)$ gravity generates phantom crossing.

For the second class (class II) of the scale factor (18) and using Eq. (19), the future event horizon R_h yields

$$R_h = a(t)\int_t^\infty \frac{\mathrm{d}t}{a(t)} = \frac{t}{(n-1)} = \sqrt{\frac{-6n^2}{T(n-1)^2}}. \tag{27}$$

Substituting Eq. (27) into (22) one can get

$$\rho_\Lambda = \frac{\delta^2(n-1)^2(-T)}{2n^2} - \lambda\left(\frac{n-1}{\sqrt{6}n}\right)^\epsilon (-T)^{\frac{\epsilon}{2}}. \tag{28}$$

Substituting Eq. (28) in the differential equation (12), i.e., $\rho = \rho_\Lambda$, gives the following solution

$$f(T) = c\sqrt{-T} - \frac{\delta^2(n-1)^2(-T)}{n^2} + \frac{2\lambda}{(\epsilon-1)}\left(\frac{n-1}{\sqrt{6}n}\right)^\epsilon (-T)^{\frac{\epsilon}{2}} \tag{29}$$

where c is the integration constant to be determined from the necessary boundary condition. In Fig. 1–6, we understand that $f(T) \nrightarrow 0$ as $T \to 0$ for the solution obtained from Eq. (29). We also observe that $f(T)$ first increases and then decreases as T increases keeping in mind that $f(T)$ takes always positive value for all values of negative T. It may be stated that the solutions obtained in Eqs. (26) and (29) are not very realistic models. Substituting Eq. (29) into (13) and using (28) we obtain the EoS parameter of the ECHDE $f(T)$ gravity in a power-law correction model as $w_\Lambda = \frac{p_\Lambda}{\rho_\Lambda}$ graphically. In Fig. 1–6, we see that the EoS parameter wholly lies in the phantom region, i.e., $w_\Lambda < -1$ always if we draw the graph of the EoS parameter with T and z using Eq. (21) respectively. So in this case, $f(T)$ gravity does not generate phantom crossing.

3.2 ECHDE in logarithmic correction

Reference [24] described the energy density of the ECHDE in a logarithmic version using the corrected entropy–area relation (2) [24],

$$\rho_\Lambda = \frac{3\delta^2}{R_h^2} + \frac{\alpha}{R_h^4}\ln(R_h^2) + \frac{\beta}{R_h^4} \tag{30}$$

where α and β are dimensionless constants of order unity and δ is a constant. In the special case $\alpha = \beta = 0$, the above equation becomes the well-known HDE density. Since only R_h is very small, the last two terms in Eq. (30) can be comparable to the first term, the corrections make sense only at the early stage of the universe. When the universe becomes large, ECHDE converts to the ordinary HDE [24].

For the first class (class I) of the scale factor (15) and using Eq. (16), and the future event horizon R_h (24) into (30), one gets

$$\rho_\Lambda = -\frac{T\delta^2(n+1)^2}{2n^2} + \frac{\alpha T^2(n+1)^2}{36n^4} \times \ln\left(-\frac{6n^2}{T(n+1)^2}\right) + \frac{\beta T^2(n+1)^4}{36n^4}. \tag{31}$$

Substituting Eq. (31) in the differential equation (12), i.e., $\rho = \rho_\Lambda$, gives the following solution:

$$f(T) = c\sqrt{-T} - \frac{T^2(n+1)^4(3\beta+2\alpha)}{162n^4} - \frac{\alpha(n+1)^4}{54n^4}T^2 \times\ln\left(-\frac{6n^2}{T(n+1)^2}\right) - \frac{\delta^2(n+1)^2}{n^2} \tag{32}$$

where c is the integration constant to be determined from the necessary boundary condition. In Fig. 7–12, we understand that $f(T) \nrightarrow 0$ as $T \to 0$ for the solution obtained from Eq. (32). We also observe that $f(T)$ first increases and then decreases as T increases keeping in mind that $f(T)$ takes always a negative value for all values of negative T. Substituting Eq. (32) into Eq. (13) and using (31) we obtain the EoS parameter of the ECHDE $f(T)$ gravity model in a logarithmic version as $w_\Lambda = \frac{p_\Lambda}{\rho_\Lambda}$ graphically. In Fig. 7–12, we see that the EoS parameter can justify the transition from the phantom state, $w_\Lambda < -1$, to the quintessence regime, $w_\Lambda > -1$, i.e., it crosses the phantom divide line $w_\Lambda = -1$ if we draw the graph of the EoS parameter with T and z using Eq. (21) respectively. So in this case, $f(T)$ gravity generates phantom crossing.

For the second class (class II) of the scale factor (18) and using Eq. (19), the future event horizon R_h (27) into (30) one can get

$$\rho_\Lambda = -\frac{T\delta^2(n-1)^2}{2n^2} + \frac{\alpha T^2(n-1)^2}{36n^4} \times \ln\left(-\frac{6n^2}{T(n-1)^2}\right) + \frac{\beta T^2(n-1)^4}{36n^4}. \tag{33}$$

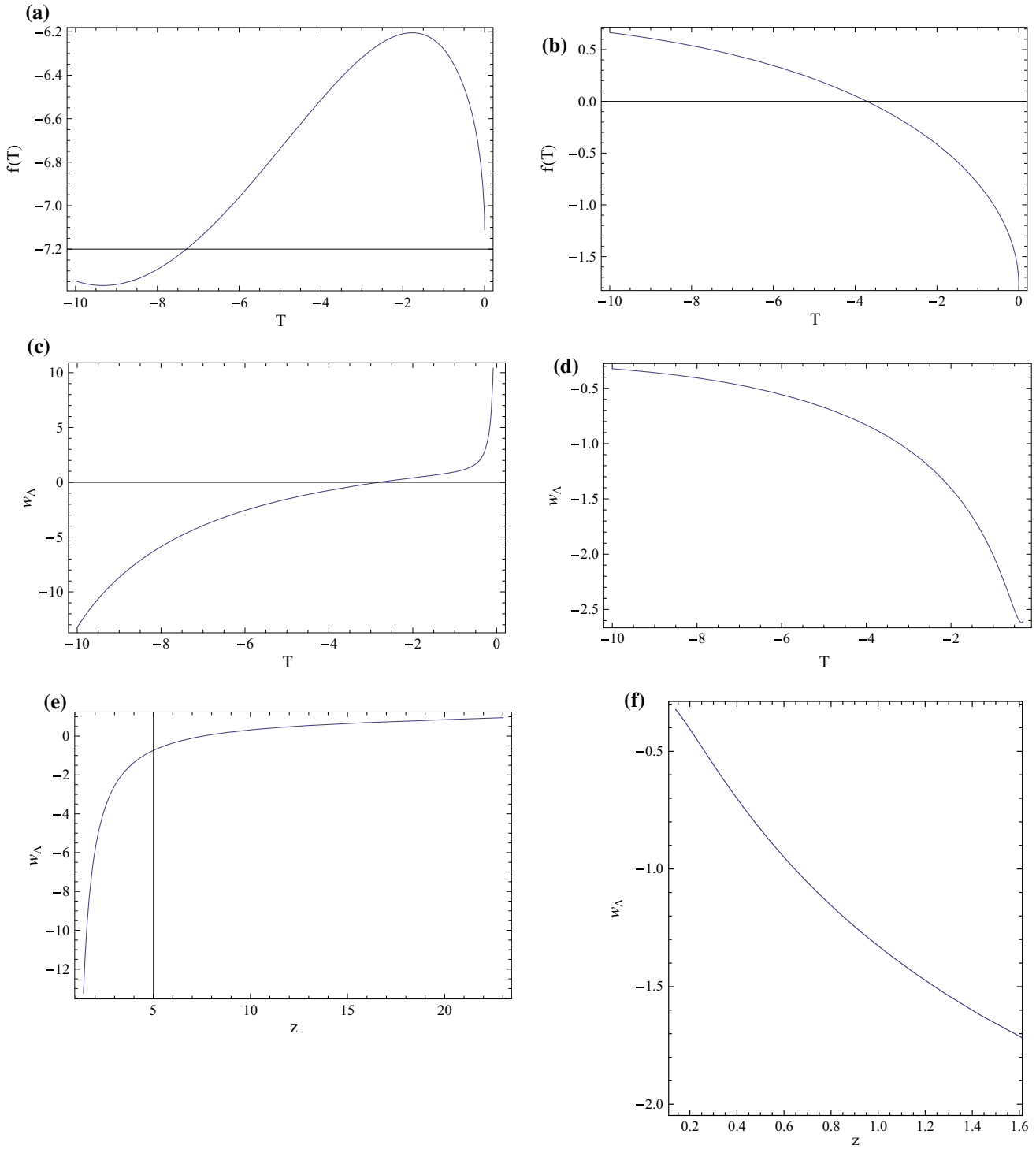

Figs. 7–12 **a, c, e** Plots of $f(T)$ and w_Λ for class I scale factor in ECHDE $f(T)$ gravity in a logarithmic correction model. **b, d, f** Plots of $f(T)$ and w_Λ for class II scale factor in ECHDE $f(T)$ gravity in a logarithmic correction model

Substituting Eq. (33) in the differential equation (12), i.e., $\rho = \rho_\Lambda$, gives the following solution

$$f(T) = c\sqrt{-T} - \frac{T^2(n-1)^4(3\beta+2\alpha)}{162n^4} - \frac{\alpha(n-1)^4}{54n^4}T^2 \times ln\left(-\frac{6n^2}{T(n-1)^2}\right) - \frac{\delta^2(n-1)^2}{n^2} \quad (34)$$

where c is the integration constant to be determined from the necessary boundary condition. In Fig. 7–12, we understand that $f(T) \nrightarrow 0$ as $T \to 0$ for the solution obtained from Eq. (34). We also observe that $f(T)$ decreases from some positive value to negative value as T increases from negative value

to zero. It may be stated that the solutions obtained in Eqs. (32) and (34) are not so-realistic models. Substituting Eq. (34) into (13) and using (33) we obtain the EoS parameter of ECHDE $f(T)$ gravity model in logarithmic version as $w_\Lambda = \frac{p_\Lambda}{\rho_\Lambda}$ graphically. In Fig. 7–12, we see that the EoS parameter can justify the transition from the quintessence state, $w_\Lambda > -1$, to the phantom regime, $w_\Lambda < -1$, i.e., it crosses the phantom divide line $w_\Lambda = -1$ if we draw the graph of the EoS parameter with T and z using Eq. (21), respectively, i.e., it crosses the line $w_\Lambda = -1$.

4 $f(T)$ reconstruction from ECNADE model in power-law and logarithmic corrections models

4.1 ECNADE in power-law correction

Reference [24] gives the energy density of the ECNADE in a power-law correction with the help of quantum corrections to the relation (1) in the setup of LQG given as

$$\rho_\Lambda = 3\delta^2\eta^{-2} - \lambda\eta^{-\epsilon}, \tag{35}$$

which is very similar to that of ECHDE in the power-law correction density (22) and R_h is replaced with the conformal time η which is given by

$$\eta = \int \frac{\mathrm{d}t}{a} = \int \frac{\mathrm{d}a}{Ha^2}. \tag{36}$$

Here ξ and ζ are dimensionless constants of order unity.

For the first class (class I) of the scale factor (15), the conformal time η with the help of Eq. (36) yields

$$\eta = \int_t^{t_s} \frac{\mathrm{d}t}{a} = -\frac{(t_s - t)^{1+n}}{a_0(1+n)} = \sqrt{\frac{(6n^2)^{n+1}}{a_0^2(-T)^{n+1}(1+n)^2}}. \tag{37}$$

Substituting Eq. (37) into (35) one can obtain

$$\rho_\Lambda = \frac{3\delta^2 a_0^2(n+1)^2(-T)^{n+1}}{(6n^2)^{n+1}} - \lambda\left\{\frac{a_0(n+1)}{6^{\frac{n+1}{2}}n^{n+1}}\right\}^\epsilon (-T)^{\frac{(n+1)\epsilon}{2}}. \tag{38}$$

Solving the differential equation (12) for the energy density (38) reduces to, i.e., $\rho = \rho_\Lambda$, gives the following solution

$$f(T) = c\sqrt{-T} - \frac{\delta^2 a_0^2(n+1)^2(-T)^{n+1}}{6^n n^{2(n+1)}(2n+1)} + \frac{2\lambda}{(n+1)\epsilon - 1}\left\{\frac{a_0(n+1)}{6^{\frac{n+1}{2}}n^{n+1}}\right\}^\epsilon (-T)^{\frac{(n+1)\epsilon}{2}} \tag{39}$$

where c is the integration constant to be determined from the necessary boundary condition. In Fig. 13–18, we understand that $f(T) \nrightarrow 0$ as $T \to 0$ for the solution obtained from Eq. (39). The function $f(T)$ decreases as T increases to zero. Substituting Eq. (39) into (13) and using (38) we obtain the EoS parameter of the ECNADE $f(T)$ gravity model in a power-law version as $w_\Lambda = \frac{p_\Lambda}{\rho_\Lambda}$ graphically. In Fig. 13–18, we see that the EoS parameter can justify the transition from the phantom state, $w_\Lambda < -1$, to the quintessence regime, $w_\Lambda > -1$, i.e., it crosses the phantom divide line $w_\Lambda = -1$ if we draw the graph of the EoS parameter with T and z using Eq. (21) respectively i.e., it crosses the line $w_\Lambda = -1$.

For the second class (class II) of the scale factor (18), the conformal time η with the help of Eq. (36) yields

$$\eta = \int_0^t \frac{\mathrm{d}t}{a} = \frac{t^{1-n}}{a_0(1-n)} = \sqrt{\frac{6^{1-n}n^{2(1-n)}}{(-T)^{1-n}a_0^2(1-n)^2}} \tag{40}$$

where $n < 1$. Substituting Eq. (40) into (35) one can obtain

$$\rho_\Lambda = \frac{3\delta^2 a_0^2(1-n)^2(-T)^{1-n}}{(6n^2)^{1-n}} - \lambda\left\{\frac{a_0(1-n)}{6^{\frac{1-n}{2}}n^{1-n}}\right\}^\epsilon (-T)^{\frac{(1-n)\epsilon}{2}}. \tag{41}$$

Solving the differential equation (12) for the energy density (41) reduces to, i.e., $\rho = \rho_\Lambda$, giving the following solution:

$$f(T) = c\sqrt{-T} - \frac{6^n\delta^2 a_0^2(1-n)^2(-T)^{1-n}}{n^{2(1-n)}(1-2n)} + \frac{2\lambda}{(1-n)\epsilon - 1}\left\{\frac{a_0(1-n)}{6^{\frac{1-n}{2}}n^{1-n}}\right\}^\epsilon (-T)^{\frac{(1-n)\epsilon}{2}} \tag{42}$$

where c is the integration constant to be determined from the necessary boundary condition. In Fig. 13–18, we understand that $f(T) \nrightarrow 0$ as $T \to 0$ for the solution obtained from Eq. (42). The function $f(T)$ decreases but keeps a negative value as T increases to zero. It may be stated that the solutions obtained in Eqs. (39) and (42) both are not realistic models. Substituting Eq. (42) into (13) and using (41) we obtain the EoS parameter of the ECNADE $f(T)$ gravity model in a power-law version, $w_\Lambda = \frac{p_\Lambda}{\rho_\Lambda}$ graphically. In Fig. 13–18, we see that the EoS parameter entirely lies in the phantom region, $w_\Lambda < -1$ if we draw the graph of the EoS parameter with T and z using Eq. (21), respectively. So in this case, $f(T)$ gravity generates phantom crossing, i.e., it does not cross the line $w_\Lambda = -1$.

4.2 ECNADE in logarithmic correction

Reference [24] gives the energy density of the ECNADE with the help of quantum corrections to the entropy–area relation (2) in the setup of LQG given as

$$\rho_\Lambda = \frac{3\alpha^2}{\eta^2} + \frac{\xi}{\eta^4}\ln(\eta^2) + \frac{\zeta}{\eta^4}, \tag{43}$$

which is very similar to that of the ECHDE density in the logarithmic version (30) and R_h is replaced with the conformal time η.

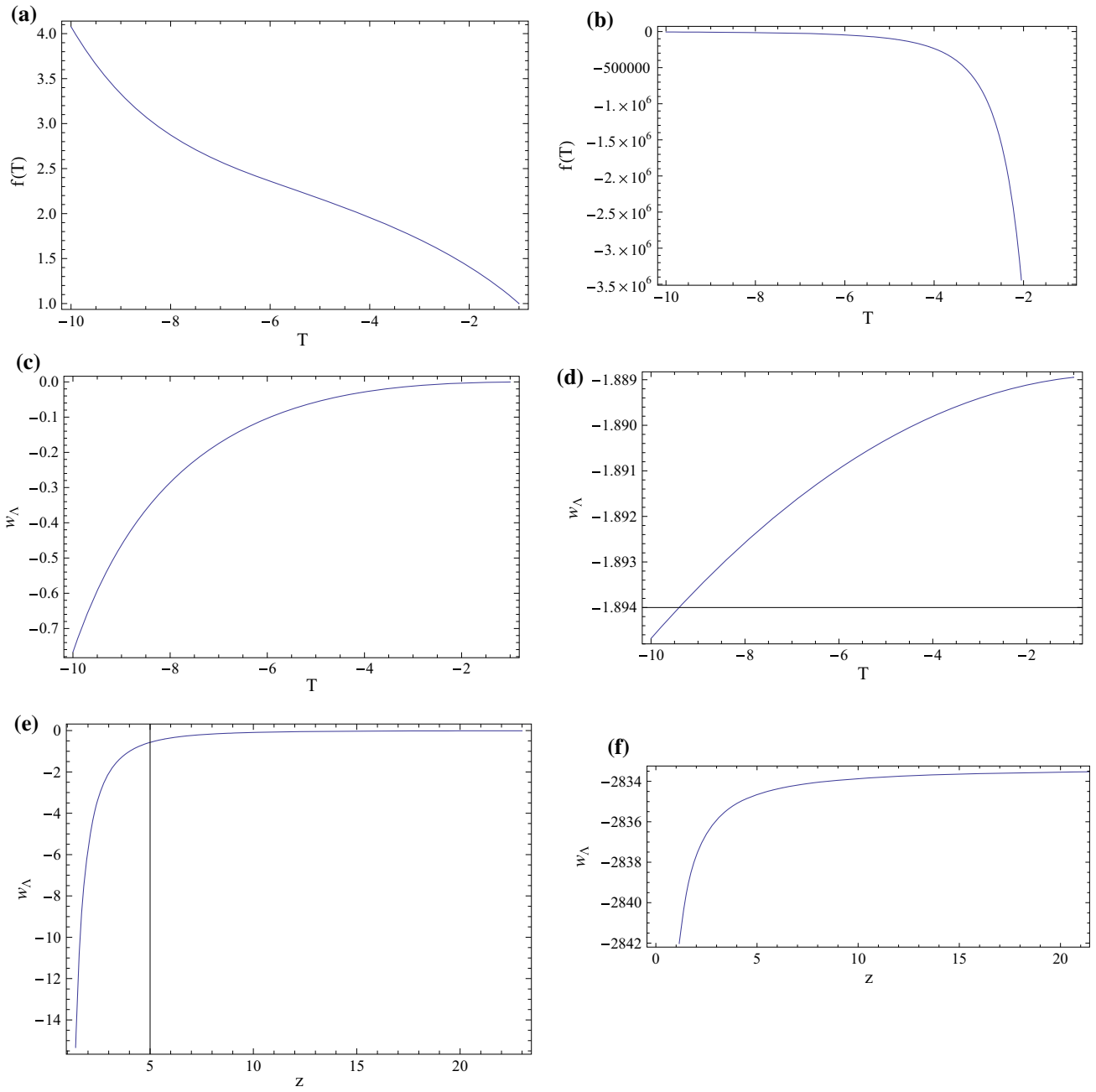

Figs. 13–18 **a, c and e** Plots of $f(T)$ and w_Λ for class I scale factor in the ECNADE $f(T)$ gravity power-law correction model. **b, d and f** Plots of $f(T)$ and w_Λ for class II scale factor in the ECNADE $f(T)$ gravity in a power-law correction model

For the first class (class I) of the scale factor (15), using the conformal time η (40), equation (43) gives

$$\rho_\Lambda = \frac{3\alpha^2 a_0^2(1+n)^2(-T)^{n+1}}{(6n^2)^{n+1}} + \frac{\xi a_0^4(1+n)^4(-T)^{2n+2}}{(6n^2)^{2n+2}} \times \ln\left(\frac{(6n^2)^{n+1}}{a_0^2(1+n)^2(-T)^{n+1}}\right) + \frac{\zeta a_0^4(1+n)^4(-T)^{2n+2}}{(6n^2)^{2n+2}}. \quad (44)$$

Solving the differential equation (12) for the energy density (44) reducing to, i.e., $\rho = \rho_\Lambda$, gives the following solution:

$$f(T) = c\sqrt{-T} - \frac{3\alpha^2(-T)^{n+1}a_0^2(1+n)^2}{(6n^2)^{n+1}(n+\frac{1}{2})} - \frac{\xi a_0^4(1+n)^4(-T)^{2n+2}}{(6n^2)^{2n+2}(2n+\frac{3}{2})}\ln\left(\frac{(6n^2)^{n+1}}{a_0^2(n+1)^2(-T)^{n+1}}\right) + \frac{(-T)^{2n+4}}{n(2n+\frac{3}{2})(2n+\frac{7}{2})}) - \frac{\zeta T^{2n+2}a_0^4(1+n)^4}{(6n^2)^{2n+2}(2n+\frac{3}{2})} \quad (45)$$

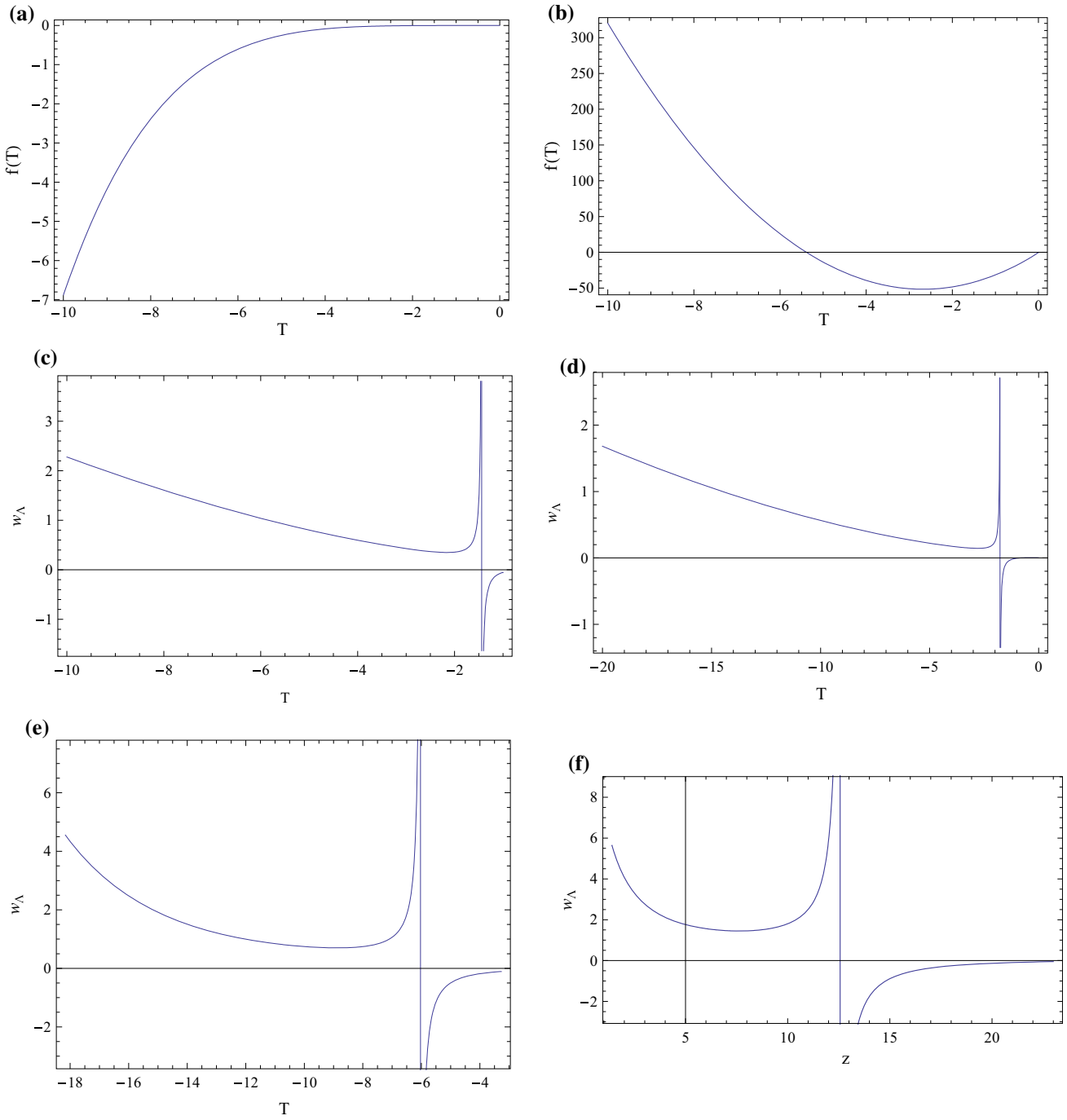

Figs. 19–24 **a, c and e** Plots of $f(T)$ and w_Λ for class I scale factor in ECNADE $f(T)$ gravity in a logarithmic correction model. **b, d and f** Plots of $f(T)$ and w_Λ for class II scale factor in ECNADE $f(T)$ gravity in a logarithmic correction model

where c is the integration constant to be determined from the necessary boundary condition. In Fig. 19–24, we understand that $f(T) \to 0$ as $T \to 0$ for the solution obtained from Eq. (45). The function $f(T)$ increases but keeps a negative value as T increases to zero. Substituting Eq. (45) into (13) and using (44) we obtain the EoS parameter of the ECNADE $f(T)$ gravity model in a logarithmic version as $w_\Lambda = \frac{p_\Lambda}{\rho_\Lambda}$ graphically. In Fig. 19–24, we see that the EoS parameter can justify the transition from the quintessence state, $w_\Lambda > -1$, to the phantom regime, $w_\Lambda < -1$, i.e., it crosses the phantom divide line $w_\Lambda = -1$ if we draw the graph of the EoS parameter with T and z using Eq. (21), respectively, i.e., it crosses the line $w_\Lambda = -1$.

For the second class (class II) of the scale factor (18), the conformal time η, see (40), Eq. (43) gives

$$\rho_\Lambda = \frac{3\alpha^2 a_0^2(1-n)^2(-T)^{1-n}}{6^{1-n}n^{2(1-n)}} + \frac{\xi a_0^4(1-n)^4T^{2-2n}}{6^{2(1-n)}n^{4(1-n)}} \times \ln\left(\frac{6^{1-n}n^{2(1-n)}}{a_0^2(1-n)^2(-T)^{1-n}}\right) + \frac{\zeta a_0^4(1-n)^4T^{2-2n}}{6^{2(1-n)}n^{4(1-n)}}. \quad (46)$$

Solving the differential equation (12) for the energy density (46) reduces to

$$f(T) = c\sqrt{-T} - \frac{3\alpha^2 a_0^2(1-n)^2(-T)^{1-n}}{6^{1-n}n^{2(1-n)}(\frac{1}{2}-n)} - \frac{\xi a_0^4(1-n)^4T^{2-2n}}{6^{2(1-n)}n^{4(1-n)}\left(\frac{3}{2}-2n\right)^2}\left(\left(\frac{3}{2}-2n\right) \times \ln\left(\frac{6^{1-n}n^{2(1-n)}}{a_0^2(1-n)^2(-T)^{1-n}}\right) + (1-n)\right) - \frac{\zeta a_0^4(1-n)^4T^{2-2n}}{6^{2(1-n)}n^{4(1-n)}(\frac{3}{2}-2n)} \quad (47)$$

where c is the integration constant to be determined from the necessary boundary condition. In Fig. 19–24, we understand that $f(T) \to 0$ as $T \to 0$ for the solution obtained from Eq. (47). The function $f(T)$ decreases from some positive value to some negative value as T increases up to a certain negative value and after that $f(T)$ increases, keeping a negative sign. It may be stated that the solutions obtained in Eqs. (45) and (47) are both realistic models. Substituting Eq. (47) into (13) and using (46) we obtain the EoS parameter of the ECNADE $f(T)$ gravity model in a logarithmic version as $w_\Lambda = \frac{p_\Lambda}{\rho_\Lambda}$ graphically. In Fig. 19–24, we see that the EoS parameter can justify the transition from the quintessence state, $w_\Lambda > -1$, to the phantom regime, $w_\Lambda < -1$, i.e., it crosses the phantom divide line $w_\Lambda = -1$ if we draw the graph of the EoS parameter with T and z using Eq. (21), respectively, i.e., it crosses the line $w_\Lambda = -1$.

5 Analysis and comparison of the reconstructed models

We now analyze an important quantity to verify the stability of ECHDE $f(T)$ in a power-law and a logarithmic correction model and ECNADE $f(T)$ in a power-law and a logarithmic correction model, named the squared speed of sound v_s^2:

$$v_s^2 = \frac{\mathrm{d}p}{\mathrm{d}\rho} = \frac{\frac{\mathrm{d}p}{\mathrm{d}T}}{\frac{\mathrm{d}\rho}{\mathrm{d}T}}. \quad (48)$$

The sign of v_s^2 is very important for checking the stability of a background evolution of the universe. In general relativity a negative sign implies a classical instability of a given perturbation [67,68]. Myung [68] has observed the always negative sign of v_s^2 for HDE for the future event horizon as we have an IR cut-off, while for a Chaplygin gas and a tachyon, there is non-negativity. Kim et al. [67] found an always negative squared speed of sound for agegraphic DE, leading to the instability of the perfect fluid for the model. Also, [69] found the ghost QCD DE model as an unstable model. Recently, Sharif and Jawad [70] have shown negative v_s^2 for the interacting new HDE.

5.1 Investigation of stability of ECHDE in power-law and logarithmic corrections

For an ECHDE $f(T)$ model in a power-law version there are two cases. For the first class (class I scale factor) we see from Fig. 25–32 that $v_s^2 > 0$ for $T \preceq -2$ and $v_s^2 < 0$ for $T \succeq -2$ and from 27 that $v_s^2 < 0$ for $z \preceq 0.1$ and $v_s^2 > 0$ for $z \succeq 0.1$ and for the second class (class II scale factor) we see from Fig. 25–32 that $v_s^2 < 0$ for the present and future epoch. So we can conclude that the ECHDE $f(T)$ model in a power-law version implies a classical stability for $T \preceq -2$, $z \succeq 0.1$ and a classical instability for $T \succeq -2$, $z \preceq 0.1$ for the first class and a classical instability of the second class of a given perturbation in general relativity.

For ECHDE $f(T)$ model in a logarithmic version there are two cases. For the first class (class I scale factor) we see from Fig. 25–32 that $v_s^2 < 0$ for the present and future epoch and for the second class (class II scale factor) we see from Fig. 25–32 that $v_s^2 < 0$ also for the present and future and future epoch. So we can conclude that the ECHDE $f(T)$ model in a logarithmic version implies a classical instability of a given perturbation in general relativity both for the first and second classes.

5.2 Investigation of stability of ECNADE in power-law and logarithmic corrections

For ECNADE $f(T)$ model in a power-law version there are also two cases. For the first class (class I scale factor) we see from Fig. 33–40 that $v_s^2 > 0$ for the present and future epoch and for the second class (class II scale factor) we see from Fig. 33–40 that $v_s^2 < 0$ for the present and future epoch. So we can conclude that the ECNADE $f(T)$ model in a power-law version implies a classical stability for the first class and a classical instability of the second class of a given perturbation in general relativity.

For the ECNADE $f(T)$ model in a logarithmic version there are also two cases. For the first class (class I scale factor) we see from Fig. 33–40 that $v_s^2 > 0$ for the present and future epoch and for the second class (class II scale factor) we see from Fig. 33–40 that $v_s^2 > 0$. So we can conclude that the ECNADE $f(T)$ model in a logarithmic version implies a classical stability both for the first and second classes.

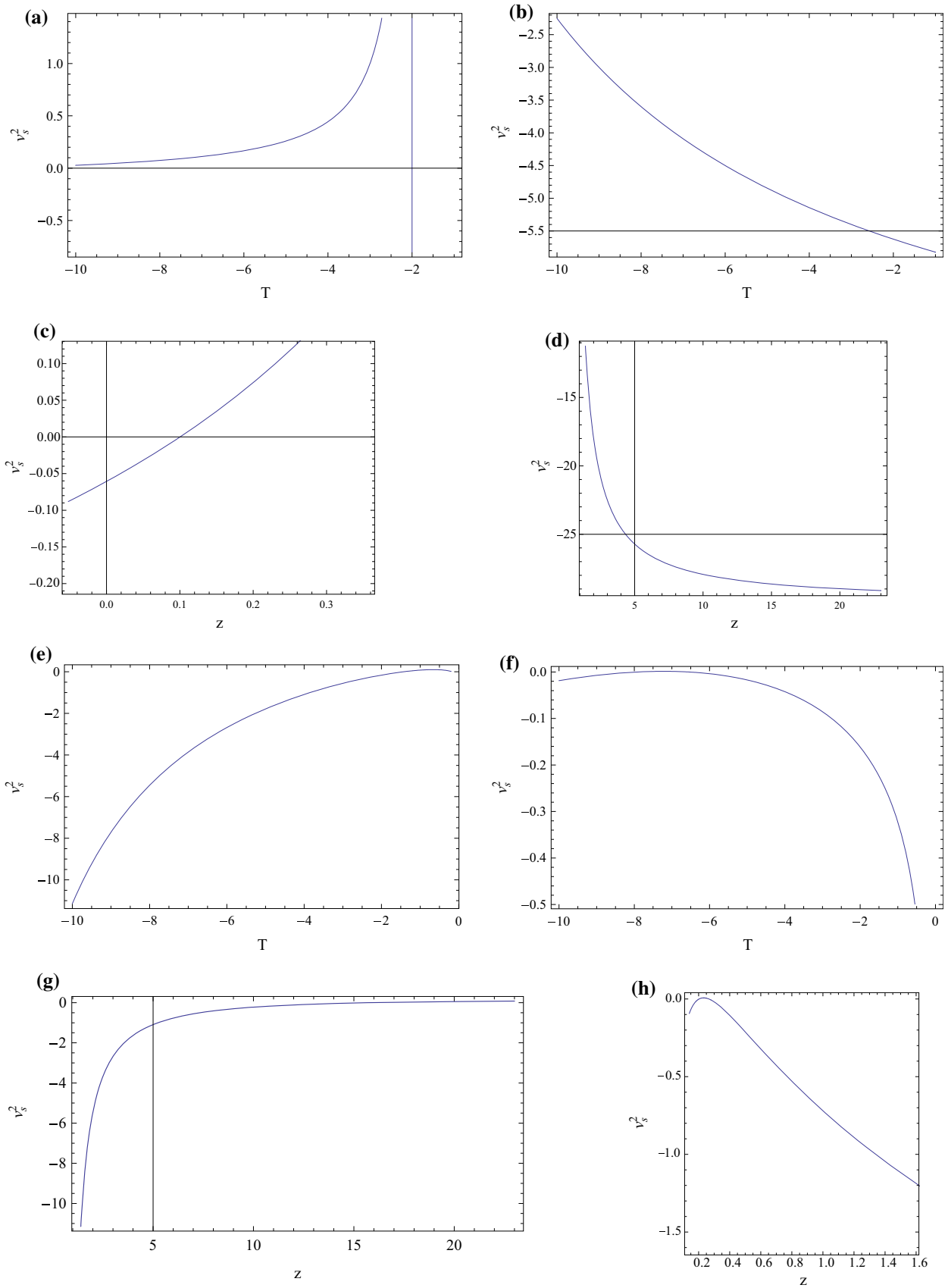

Figs. 25–32 **Figs. 25–28** Plots of v_s^2 for class I and class II scale factors in ECHDE $f(T)$ gravity model in a power-law correction. **Figs. 29–32** Plots of v_s^2 for class I and class II scale factors in ECHDE $f(T)$ gravity model in a logarithmic correction

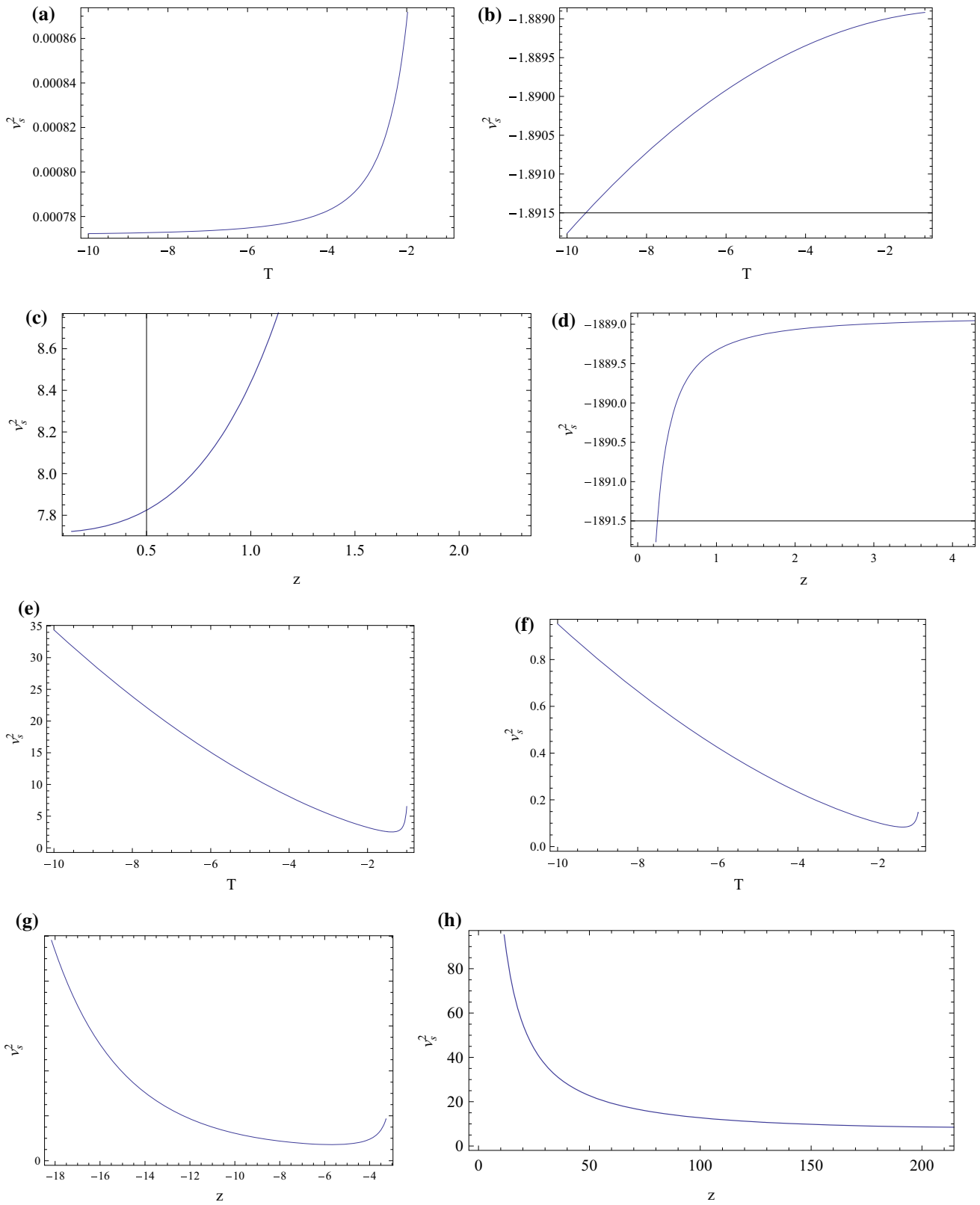

Figs. 33–40 **Figs. 33–36** Plots of v_s^2 for class I and class II scale factors in ECNADE $f(T)$ gravity model in a power-law correction. **Figs. 37–40** Plots of v_s^2 for class I and class II scale factors in ECNADE $f(T)$ gravity model in a logarithmic correction

6 Concluding remarks

In this work, we have assumed the $f(T)$ modified gravity theory in the background of a flat FRW universe. We found the modified Friedmann equations and then, from the equations, we found the effective energy density and pressure for $f(T)$ modified gravity theory. Modified gravity gives a natural unification of the early-time inflation and late-time acceleration. We have assumed two types of power-law forms of scale factor, the first class (class I) has a future singularity and the second class (class II) has an initial singularity. In the framework of an $f(T)$ modified gravity model, four types of dark energy have been considered: (1) the entropy-corrected holographic dark energy (ECHDE) in power-law version, (2) the entropy-corrected holographic dark energy (ECHDE) in logarithmic version, (3) the entropy-corrected new agegraphic dark energy (ECNADE) in a power-law version, and (4) the entropy-corrected new agegraphic dark energy (ECNADE) in a logarithmic version, where R_h is assumed to be the future event horizon and η is assumed to be conformal time. Using the two classes of scale factors, the unknown function $f(T)$ has been found in terms of T for the ECHDE and ECNADE models in power-law and logarithmic versions. The corresponding equation of states have also been generated. For the cases of ECHDE and ECNADE in power-law and logarithmic versions the natures of $f(T)$ vs. T are shown in Figs. 1–6, 7–12, 13–18 and 19–24. For the cases of ECHDE in a power-law version (class I) and logarithmic version (class I and II), ECNADE in a power-law version (class I) and logarithmic version (class I and II), the equation of state parameter w_Λ is shown in Figs. 1–6, 7–12, 13–18 and 19–24, whereas in Figs. 1–6 and 19–24, the EoS parameter is divergent at $T = -1, -10, z = 0, 25$; $T = -4, z = -6$, and at $T = -2$, $z = 13.5$. For the cases of ECHDE in a power-law version (class II) and ECNADE in a power-law version (class II) the equation of state parameter w_Λ is shown in Figs. 1–6 and 13–18. From the figures we see that these models lie entirely in the phantom region. It should be mentioned that Karami et al. [59] have investigated the $f(T)$ reconstructions for the HDE, NADE models, and logarithmic versions of the ECHDE, ECNADE models only, and for these models we got the similar expressions of $f(T)$ but we have in detail studied the results graphically. To examine the stability test for all the reconstructing models, we have investigated the signs of the square of the velocity of sound. For ECHDE model in a power-law version , we have concluded from Fig. 25–32, that the corresponding model is a classical stable for $T \leq -2$, $z \geq 0.1$, and classically unstable for $T \geq -2$, $z \leq 0.1$ for the first class and from Fig. 25–32 the corresponding model is a classically unstable for second class of a given perturbation in general relativity. For the ECHDE model in a logarithmic version, we have concluded from Fig. 25–32 that the corresponding models are unstable both for class I and class II. On the other hand, for the ECNADE model in a power-law version (class I), we have seen from Fig. 33–40 that the corresponding model is stable and for the ECNADE model in a power-law version (class II) we have seen from Fig. 33–40 that the corresponding model is unstable. Again for ECNADE in a logarithmic version (class I and II), we have seen from Fig. 33–40 that the corresponding models are stable. Thus we may conclude that our reconstructed ECHDE model (class I), ECNADE model in a power-law version (class I) and logarithmic version (class I and II) are more realistic (and classically stable) than the other models (classically unstable) discussed.

Acknowledgments One of the authors (UD) is thankful to IUCAA, Pune, India, where part of the work was carried out, for warm hospitality.

Funded by SCOAP[3].

References

1. S.J. Perlmutter et al., Nature **391**, 51 (1998)
2. A.G. Riess et al. [Supernova Search Team Collaboration], Astron. J. **116**, 1009 (1998)
3. E.J. Copeland, M. Sami, S. Tsujikawa, Int. J. Mod. Phys. D **15**, 1753 (2006)
4. S. Tsujikawa, Lect. Notes phys **800**, 99 (2010)
5. V. Sahni, A. Starobinsky, Int. J. Mod. Phys. D **15**, 2105 (2006)
6. M. Seikel, C. Clarkson, M. Smith, JCAP D **06**, 036 (2012)
7. C. Clarkson, C. Zunckel, Phys. Rev. Lett. **104**, 211301 (2010)
8. X.M. Liu, W.B. Liu, Astrophys. Space Sci. **334**, 203 (2011)
9. K. Enqvist, S. Hannested, M.S. Sloth, JCAP **2**, 004 (2005)
10. X. Zhang, Int. J. Mod. Phys. D **14**, 1597 (2005)
11. D. Pavon, W. Zimdahl. arXiv:hep-th/0511053
12. W. Fischler, L. Susskind. arXiv:hep-th/9806039
13. G. 't Hooft (1993). arXiv:gr-qc/9310026
14. A. Cohen, D. Kaplan, A. Nelson, Phys. Rev. Lett **82**, 4971 (1999)
15. M. Li, Phys. Lett. B **603**, 1 (2004)
16. K. Enqvist, M.S. Sloth, Phys. Rev. Lett. **93**, 221302 (2004)
17. Q.-G. Huang, Y.-G. Gong, JCAP **08**, 006 (2004)
18. Y.-G. Gong, Phys. Rev. D **70**, 064029 (2004)
19. E. Elizalde, S. Nojiri, S.D. Odintsov, P. Wang, Phys. Rev. D **71**, 103504 (2005)
20. X. Zhang, F.-Q. Wu, Phys. Rev. D **72**, 043524 (2005)
21. N. Radicella, D. Pavon, Phys. Lett. B **691**, 121 (2010)
22. A. Sheykhi, M. Jamil, Gen. Relativ. Gravit. **43**, 2661 (2011)
23. S. Das, S. Shankaranarayanan, S. Sur, Phys. Rev. D **77**, 064013 (2008)
24. H. Wei, Commun. Theor. Phys. **52**, 743 (2009)
25. R. Banerjee, B.R. Majhi, Phys. Lett. B **662**, 62 (2008)
26. S.K. Modak, Phys. Lett. B **671**, 167 (2009)
27. H.M. Sadjadi, M. Jamil, Eur. Lett. **92**, 69001 (2010)
28. S.-W. Wei, Y.-X. Liu, Y.-Q. Wang, H. Guo. arXiv:1002.1550 [SPIRES]
29. R.G. Cai, Phys. Lett. B **657**, 228 (2007)
30. H. Wei, R.G. Cai, Phys. Lett. B **660**, 113 (2008)

31. K. Karami, M.S. Khaledian, JHEP **03**, 086 (2011)
32. K. Karami, A. Sorouri, Phys. Scr. **82**, 025901 (2010)
33. K. Karami et al., Gen. Relativ. Gravit. **43**, 27 (2011)
34. M.U. Farooq, M. Jamil, M.A. Rashid, Int. J. Theor. Phys. **49**, 2278 (2010)
35. M. Malekjani, A. Khodam-Mohammadi. arXiv:1004.1017 [SPIRES]
36. S. Capozziello, Curvature quintessence. Int. J. Mod. Phys. D **11**, 483 (2002)
37. S. Nojiri, S.D. Odintsov, Phys. Rev. D **74**, 086005 (2006)
38. S. Nojiri, S.D. Odintsov, Phys. Rev. D **74**, 086005 (2006)
39. R. Myrzakulov, D. Sáez-Gómez, A. Tureanu, Gen. Relativ. Gravit. **43**, 1671 (2011)
40. A. Banijamali, B. Fazlpour, M.R. Setare, Astrophys. Space Sci. **338**, 327 (2012)
41. E. Kiritsis, G. Kofinas, Nucl. Phys. B **821**, 467 (2009)
42. S. Nojiri, S.D. Odintsov, Phys. Lett. B **631**, 1 (2005)
43. B. Li, J.D. Barrow, Phys. Rev. D **76**, 044027 (2007)
44. Y.-F. Cai, S.-H. Chen, J.B. Dent, S. Dutta, E.N. Saridakis, Class. Quantum Gravity **28**, 215011 (2011)
45. R. Ferraro, F. Fiorini, Phys. Rev. D **75**, 084031 (2007)
46. B. Li, T.P. Sotiriou, J.D. Barrow, Phys. Rev. D **83**, 064035 (2011)
47. T.P. Sotiriou, B. Li, J.D. Barrow, Phys. Rev. D **83**, 104030 (2011)
48. K. Bamba, C.-Q. Geng, J. Cosmol. Astropart. Phys. **11**, 8 (2011)
49. M. Jamil, K. Yesmakhanova, D. Momeni, R. Myrzakulov, Central Eur. J. Phys. (2012) (Online first)
50. M. Jamil, D. Momeni, R. Myrzakulov, P. Rudra, J. Phys. Soc. Jpn. **181**, 11 (2012)
51. A. Khodam-Mohammadi, P. Majari, M. Malekjani, Astrophys. Space Sci. **331**, 673–677 (2011)
52. A. Jawad, S. Chattopadhyay, A. Pasqua, Eur. Phys. J. Plus **128**, 88 (2013)
53. S. Chattopadhyay, A. Pasqua, Astrophys. Space Sci. **344**, 269–274 (2013)
54. U. Debnath, Adv. High Energy Phys. **2014**, 475862 (2014)
55. M.H. Daouda, M.E. Rodrigues, M.J.S. Houndjo, Eur. Phys. J. C. **72**, 1893 (2012)
56. M.U. Farooq, M. Jamil, D. Momeni, R. Myrzakulov, Can. J. Phys. **91**, 703–708 (2013). arXiv:1306.1637. [astro-ph.CO]
57. K. Karami, M.S. Khaledian, JHEP **1103** 086 (2011). arXiv:1004.1805 [v3 gr-qc]
58. U. Debnath, Astrophys. Space Sci. **355**, 405–411 (2015)
59. K. Karami, A. Abdolmaleki, Res. Astron. Astrophys. **13**, 757 (2013)
60. V.C. De Andrade, L.C.T. Guillen, J.G.Pereira, Nov 2000, Talk given at conferrence C00-07-02. arXiv:gr-qc/0011087 [v1]
61. G. Bengochca, R. Ferraro, Phys. Rev. D **79**, 124019 (2009)
62. E.V. Linder, Phys. Rev. D **81**, 127301 (2010)
63. Y.-F. Cai, S.-H. Chen, J.B. Dent, S. Dutta, E.N. Saridakis. arXiv:1104.4349 [v2]
64. M.R. Setare, F. Darabi. arXiv:1110.3962 [v1 physics.gen-ph]
65. M.R. Setare, M.J.S. Houndjo, arXiv:1111.2821 [physics.gen-ph]
66. M.R. Setare, Int. J. Mod. Phys. D **12**, 2219 (2008)
67. K.Y. Kim, H.W. Lee, Y.S. Myung, Phys. Lett. B **660**, 118 (2008)
68. Y.S. Myung, Phys. Lett. B **652**, 223 (2007)
69. E. Ebrahimi, A. Sheykhi, Int. J. Mod. Phys. D **20**, 2369 (2011)
70. M. Sharif, A. Jawad, Eur. Phys. C **72**, 2097 (2012)